

RADIATIVE PION CAPTURE IN  $^{12}\text{C}$ 

James A. Bistirlich, Kenneth M. Crowe, Anthony S. L. Parsons,\* P. Skarek,† and P. Truøel‡  
*Lawrence Radiation Laboratory, University of California, Berkeley, California 94720*

(Received 8 June 1970)

The spectrum of high-energy gamma rays following the capture of negative pions in  $^{12}\text{C}$  was measured with high resolution. The observed structure in the giant resonance region is the first direct experimental proof of the influence of collective excitations in radiative pion capture. This supports recent theories concerning the analogy between this process and muon capture.

Using the hypothesis of partial conservation of axial current (PCAC), it can be shown<sup>1</sup> that the matrix elements for radiative pion capture, i.e., the process  $\pi^- N(A, Z) \rightarrow \gamma N'(A, Z-1)$ , are linked to the axial matrix elements appearing in the weak interactions of  $\mu$  capture and  $\beta$  decay. In the limit of vanishing pion mass, the two amplitudes are proportional. The formal analogy in the impulse approximation between the effective Hamiltonians in the axial part of the  $\mu$  capture and radiative  $\pi$  capture<sup>2</sup> allows one to transfer the well-established theory for  $\mu$  capture to the latter process. It was realized<sup>3</sup> that in order to explain the total capture rates,  $\mu$  capture must proceed predominantly through the excitations of collective states in the residual nucleus, namely, the  $T_3 = -1$  analogous states to the giant resonances seen in photoabsorption and inelastic electron scattering. The excitation of these collective states has been inferred<sup>4</sup> in  $\mu$  capture on  $^{16}\text{O}$  by observing the low-energy nuclear  $\gamma$  rays from the de-excitation of the residual nucleus after the emission of an energetic neutrino. In the case of pion capture, an energetic  $\gamma$  ray is emitted instead of a neutrino. Predictions<sup>5</sup> based on the assumptions mentioned earlier show a considerable fine structure in the high-energy  $\gamma$  spectra. The data<sup>6</sup> available do not allow a significant check to be made on the predictions, mainly because of insufficient resolution. The only direct test of the analogy of the matrix elements, by comparing  $\mu^-$  and  $\pi^-$  capture rates in  $^6\text{Li}$  to the  $^6\text{He}$  ground state,<sup>7</sup> confirmed the theoretical estimates, but within an error of approximately 25%.

In our experiment<sup>8</sup> we have measured the high-energy  $\gamma$  spectrum from absorption in carbon using a  $\gamma$ -ray pair spectrometer with  $\sim 1.5\%$  resolution. The experimental setup is shown in Fig. 1. A  $\pi^-$  beam from the 184-in. cyclotron was stopped in a 2.5-cm carbon target. The spectrometer was placed to detect  $\gamma$  rays at  $90^\circ$  to the incident  $\pi$  direction. It consisted of two  $46 \times 91$ -cm C magnets combined with a common pole tip to give an

analyzing area of 218 cm in length and a 33-cm gap. A field of 10 kG was achieved and was measured to an accuracy of 0.2% throughout the volume. The  $\gamma$  rays were converted in a 0.03 radiation-length gold foil at 109 cm from the target. The directions of electron-positron pairs at entry and exit were measured using six arrays of four-gap spark chambers as shown in Fig. 1. To minimize multiple scattering and energy loss the spark chambers were constructed of low-mass material (20 mg per gap).<sup>9</sup> Tracks were recorded photographically and have been measured on semiautomatic measuring machines. The trigger for an event was a stopped pion and a coincidence between any two nonadjacent pairs of counters out of the six mounted in front of the magnet (see Fig. 1). In the analysis an iterative tracking procedure was used to obtain the best-fit momenta to the orbits of the electron and positron.

In order to check the calculated resolution and efficiency of the spectrometer, we performed a calibration experiment using liquid hydrogen.

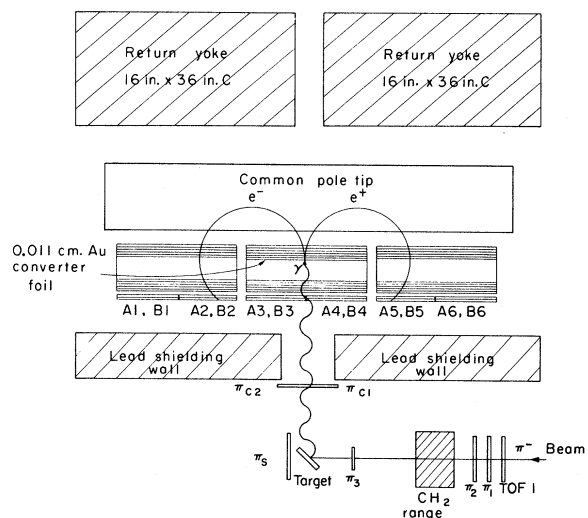


FIG. 1 Experimental layout. The mirror system for photography of the spark chambers and details of the magnet coils are omitted for clarity. The trigger for an event was  $\pi_1 \pi_2 \pi_3 \pi_4 \pi_5 \pi_6 A_i B_j A_k B_l$ ,  $i \neq k, k \pm 1$ .

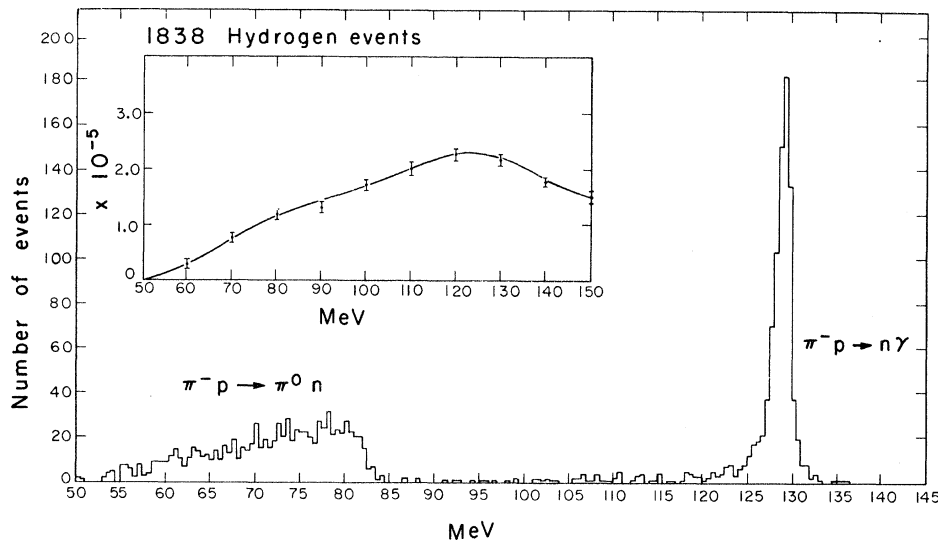


FIG. 2 Energy spectrum of  $\gamma$  rays from  $\pi^-$  capture in hydrogen. The insert shows the efficiency computed from the Monte Carlo program. The smooth curve was used in the analysis.

The reaction  $\pi^- p \rightarrow n\gamma$  with pions at rest gives a monochromatic  $\gamma$  ray of 129.4 MeV. This provides a measurement of the resolution as well as an independent calibration of the energy scale. The spectrum of  $\gamma$  rays produced in charge exchange ( $\pi^- p \rightarrow n\pi^0 \rightarrow n\gamma\gamma$ ) serves as a check on the low-energy end of the efficiency curve. The resulting spectrum is shown in Fig. 2 together with the energy-dependent efficiency as obtained from a Monte Carlo calculation; this included for electrons or positrons below 25 MeV the energy-dependent efficiency observed in the data. We find a Panofsky ratio of  $1.44 \pm 0.16$  in agreement with the accepted value of  $1.53 \pm 0.05$ . The absolute yield of the two reactions agrees with the expected one within the statistical error of 10%. The resolution at 129 MeV is 2.0 MeV full width at half-maximum and agrees with the calculated value obtained from the Monte Carlo program when measurement errors are included.

The branching ratio for radiative  $\pi$  capture (about 2%), combined with the acceptance of the spectrometer, limited our data sample for carbon to 6500 events obtained in  $\sim 30$  h beam time. The resulting, uncorrected spectrum is displayed in Fig. 3(a). There are three clearly resolved peaks around 124, 119, and 117 MeV superimposed on a continuum which extends to the low-energy cutoff of our spectrometer. The energies of the observed peaks, when corrected for energy loss in the converter and the spark chambers, correspond to  $\gamma$  energies 124.7, 120.3, and 117.0 MeV. The highest peak can be associated with a transition to the  $^{12}\text{B}$  ground state ( $E_\gamma = 125.0$ ).

This level has its analog in the  $T=1, J=1^+$  level at 15.1 MeV in  $^{12}\text{C}$ . The other two peaks can be interpreted as the  $\Delta T=-1$  analogous states to the excitations at 19.5 and the giant resonance at 22.5 MeV, as seen in inelastic electron scattering on carbon<sup>10</sup> and in photoabsorption. In order to compute the capture rate to these different states, the shape of the nonresonant background has to be known.

In an earlier paper<sup>8</sup> we have shown that neither simple phase space with a  $^{11}\text{B}n\gamma$  final state nor the Fermi-gas model can reproduce the shape of the spectrum at lower  $\gamma$  energies. We have used a pole model<sup>11</sup> to describe the direct-emission process, which was recently proposed as a competing mechanism to the resonance absorption. The capture occurs on an individual proton in the nucleus and is described by the graph shown in Fig. 3(a). The calculation contains, besides the normalization, another free parameter, the  $Q$  value of the  $^{12}\text{C} \rightarrow ^{11}\text{B}^* + p$  vertex point. We have chosen a value of 17.3 MeV, corresponding to the  $^{11}\text{B}$  ground state.

We have obtained parameters for the three peaks and the continuum by simultaneously fitting to the data a function given by the pole model plus three noninterfering Breit-Wigner resonances. The free parameters are the energies, widths, and amplitudes of the peaks, and the normalization of the continuum. Before fitting, the experimental resolution has been folded into the theoretical curve and allowance has been made for the efficiency and for an in-flight background ( $\sim 10\%$ ). This background has been esti-

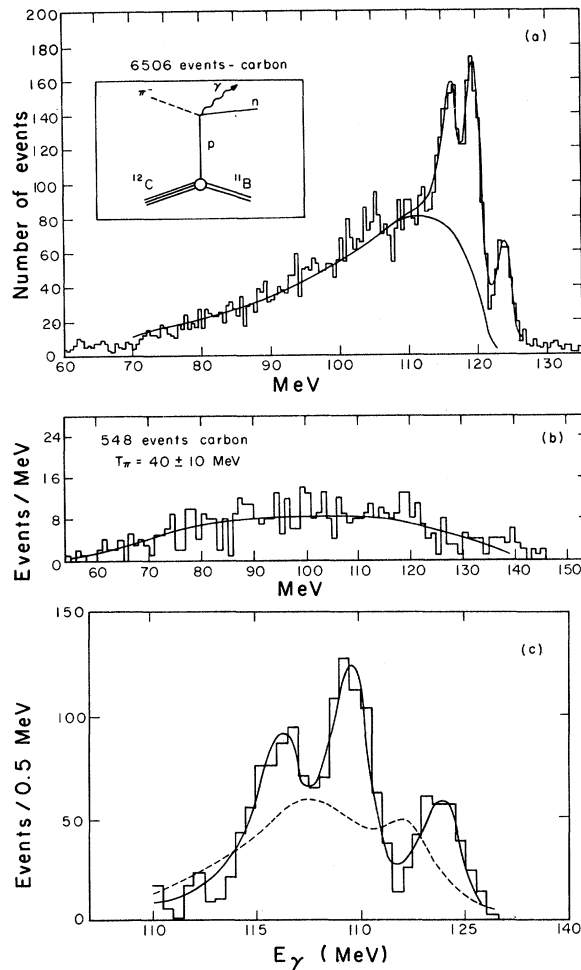


FIG. 3 (a) Uncorrected energy spectrum of  $\gamma$  rays from  $\pi^-$  capture in carbon. The smooth curve is a fitted function using three Breit-Wigner forms plus a pole model for the continuum in which allowance is made for the efficiency and an in-flight background. The contribution of the pole model beneath the peaks is also shown. (b) Energy spectrum for pions with a mean kinetic energy of 40 MeV. The smooth curve is hand drawn and is used for subtraction of in-flight background for stopped-pion data. (c) Spectrum with the pole model subtracted. The smooth curve is the best fit and the dashed curve is the prediction by Kelly and Überall (Ref. 5) using the Arima model for the giant-resonant states (normalized for the number of captured pions and folded with the experimental resolution and efficiency).

mated using data taken at 40-MeV pion kinetic energy [see Fig. 3(b)] and normalized assuming that events above 130 MeV arise from in-flight pions. In Fig. 3(c) we show the data with the pole-model prediction subtracted and the best fit to the three peaks. The parameters of the peaks

are given in Table I; the overall  $\chi^2$  for the best fit is 150 for 103 degrees of freedom ( $70 \leq E_\gamma \leq 126$  MeV). It should be emphasized that we cannot discount the possibility of the pole model being wrong and that further structure exists below 117 MeV. A more sophisticated approach to the description of the continuum would include a more complete treatment of the initial state of the proton in the nucleus.<sup>12</sup>

We compare our subtracted spectrum with predictions by Kelly and Überall<sup>5</sup> who computed the matrix elements using two different particle-hole models<sup>13,14</sup> for the nuclear levels involved. We have divided their capture rates by the measured total capture rates and weighted them by the relative probability for absorption from a  $1s$  orbit and a  $2p$  orbit.<sup>15</sup> For both models the total theoretical capture rates with excitation of particle-hole states agree with the experimental values within the errors. The theoretical spectrum for the first model,<sup>13</sup> folded with the experimental resolution and efficiency, is given in Fig. 3(c). The agreement, mainly with regard to the positions of the dominant states, is poor. Since for the alternative model of Lewis and Walecka<sup>14</sup> the widths are not given, we compare in Table I the experimental rates with the theoretical predictions. The location of the levels in this case is predicted well. The experimental errors quoted are statistical. Possible systematic errors arise from the inefficiencies in the spark chambers, determination of the number of pions stopped in the target, and the evaluation of the product of efficiency and solid angle. An estimate of these errors and the comparison with the calibration run set an upper limit of about 10% for the combination of all these quantities. The uncertainty about the shape of the nonresonant background could, of course, produce a larger effect. The capture rates for the level around 19 MeV disagree by 30%; for the giant-dipole region they agree very well. It should be mentioned that the rescattering terms and quadrupole excitations in the above theoretical capture rates have been neglected.<sup>16</sup>

Since the threshold for  $^{12}\text{B} \rightarrow ^{11}\text{B} + n$  lies 3.4 MeV higher than the  $^{12}\text{B}$  ground state, the measured capture rate to this state is free of any uncertainty in the continuum subtraction. Since the  $\mu$ -capture rate has been measured, the form factors for inelastic electron scattering are known, and the  $ft$  value for the  $\beta$  decay to the  $^{12}\text{C}$  ground state has been measured, this transition

Table I. Experimental and theoretical parameters for observed states in  $\pi^-$  capture in carbon.

$E_\gamma$ , expt <sup>a</sup> (MeV)	$\Gamma$ , expt (MeV)	$E(^{12}\text{B})$ , expt <sup>a</sup> (MeV)	$E(^{12}\text{C})$ , expt <sup>a</sup> (MeV)	$E(^{12}\text{C})(J^\pi)$ , theor <sup>b</sup> (MeV)	$\frac{\Delta\pi, \text{rad}}{\Delta\pi, \text{tot}}$ , expt (%)	$\frac{\Delta\pi, \text{rad}}{\Delta\pi, \text{tot}}$ , theor <sup>b</sup> (%)
$124.65 \pm 0.05$	$0.31 \pm 0.08$	0.34	15.4	15.1 (1 <sup>+</sup> )	$0.097 \pm 0.009$	
$120.25 \pm 0.05$	$0.45 \pm 0.12$	4.80	19.9	19.1 (2 <sup>-</sup> )	$0.195 \pm 0.017$	$0.146 \pm 0.013$
$116.90 \pm 0.11$	$1.09 \pm 0.13$	8.19	23.3	21.6 (1 <sup>-</sup> )	$0.168 \pm 0.015$	$0.026 \pm 0.002$
				23.3 (1 <sup>-</sup> )		$0.089 \pm 0.007$
				22.3 (2 <sup>-</sup> )		$0.057 \pm 0.005$
Particle-hole states					$0.363 \pm 0.023$	$0.407 \pm 0.034^b$
Pole contribution					$1.571 \pm 0.114$	
					$2.03 \pm 0.12$	$2.0^d$ $2.3^e$
					$1.60 \pm 0.1^c$	

<sup>a</sup>All errors quoted are the statistical ones only; the possible systematic error in the calibration of the energy scale is 0.5 MeV.

<sup>b</sup>Kelley and Überall's prediction (Ref. 5) using model of Ref. 10.

<sup>c</sup>Ref. 6.

<sup>d</sup>Ref. 2b.

<sup>e</sup>Ref. 2c.

is well suited for a check of the relation between these different processes in an almost model-independent way.<sup>17</sup> A theoretical calculation seems, therefore, highly desirable.

The general qualitative agreement between theory and experiment at the present stage is gratifying. It can be concluded that the expected analogy between  $\mu$  and  $\pi$  capture is indeed fulfilled, and that radiative pion absorption does offer a powerful tool to study the collective excitations in nuclei.

The authors wish to express their gratitude to their industrious scanners and to the cyclotron crew under James Vale. One of us (P.T.) gratefully acknowledges the support of the Swiss Institute for Nuclear Research and the Lawrence Radiation Laboratory during his stay in Berkeley. This work was supported in part by the U. S. Atomic Energy Commission.

\*Now at Rutherford Laboratory, Chilton, Didcot, Berkshire, England.

†Permanent address: CERN, Geneva, Switzerland.

‡Now at Physics Department, University of California, Los Angeles, Calif.

<sup>1</sup>M. Ericson and A. Figureau, Nucl. Phys. **B3**, 609 (1967); M. Pietschmann, L. R. Fulcher, and J. M. Eisenberg, Phys. Rev. Lett. **19**, 1259 (1967); D. Grifiths and C. W. Kim, Nucl. Phys. **B4**, 309 (1968).

<sup>2a</sup>A. Fujii and D. J. Hall, Nucl. Phys. **32**, 102 (1962).

<sup>2b</sup>J. Delorme and T. E. O. Ericson, Phys. Lett. **21**, 98 (1966).

<sup>2c</sup>D. K. Anderson and J. M. Eisenberg, Phys. Lett. **22**, 164 (1966).

<sup>3</sup>L. L. Foldy and J. D. Walecka, Nuovo Cimento **34**, 1026 (1964).

<sup>4</sup>S. N. Kaplan, R. V. Pyle, L. E. Temple, and G. F. Valby, Phys. Rev. Lett. **22**, 795 (1969).

<sup>5</sup>F. J. Kelly and H. Überall, Nucl. Phys. **A118**, 302 (1968).

<sup>6</sup>H. Davies, H. Muirhead, and J. N. Woulds, Nucl. Phys. **78**, 673 (1966).

<sup>7</sup>J. P. Deutsch, L. Grenacs, P. Igo-Kemenes, P. Lipnik, and P. C. Macq, Phys. Lett. **26B**, 315 (1968).

<sup>8</sup>Preliminary results are given in *Proceedings of the Third International Conference on High Energy Physics and Nuclear Structure, New York, 1969*, edited by S. Devons (Plenum, New York, 1970).

<sup>9</sup>G. Schnurmacher *et al.*, Nucl. Instrum. Methods **60**, 89 (1968).

<sup>10</sup>T. W. Donnelly, J. D. Walecka, I. Sick, and E. B. Hughes, Phys. Rev. Lett. **21**, 1196 (1968).

<sup>11</sup>L. G. Dakhno and Yu D. Prokoshkin, Yad. Fiz. **7**, 565 (1968) [Sov. J. Nucl. Phys. **7**, 351 (1968)].

<sup>12</sup>D. K. Anderson, Bull. Amer. Phys. Soc. **15**, 569 (1970).

<sup>13</sup>M. Kamimura, K. Ikeda, and A. Arima, Nucl. Phys. **A95**, 129 (1967).

<sup>14</sup>F. H. Lewis and J. D. Walecka, Phys. Rev. **133**, B849 (1964).

<sup>15</sup>Taking the weighted average of all experimental measurements for the widths of the  $2p-1s$  pionic transition, we obtain  $\Gamma_{2p \rightarrow 1s} = 3.12 \pm 0.16$  MeV. [See R. Kunselman, thesis, University of California at Berkeley Report No. UCRL 18654 (unpublished).] Averaging the yield for this transition gives  $0.076 \pm 0.009$ , leading to  $\Gamma_{2p} = 1.03 \pm 0.12$  eV and relative probabilities for the capture from the  $1s$  and the  $2p$  level of  $0.123 \pm 0.014$  and  $0.887 \pm 0.014$ , respectively. [M. Koch *et al.*, Phys. Lett. **29B**, 140 (1969).]

<sup>16</sup>For <sup>16</sup>O it has been shown that the corrections from the rescattering terms can be as much as 40% [R. Guy and J. M. Eisenberg, Nucl. Phys. **B11**, 601 (1969), and that the quadrupole excitations are quite impor-

tant [J. D. Murphy *et al.*, Phys. Rev. Lett. **19**, 714 (1967)].

<sup>17</sup>L. L. Foldy and J. D. Walecka, Phys. Rev. **B140**, 1339 (1965).

## SOLID-STATE CONVECTION ON JUPITER\*

R. Smoluchowski

*Princeton University, Princeton, New Jersey 08540*

(Received 27 May 1970)

Solid-state convective motions in the molecular-hydrogen mantle of Jupiter are evaluated and the resulting heat flux through the solid (and liquid) layers compared with observations.

Various models of Jupiter<sup>1-3</sup> lead to a conductive or convective heat flow in the planet's metallic-hydrogen core and to a convective heat transport in the external molecular-hydrogen layers. It is only recently, however, that the pertinent physical properties of the liquid layer in the supercritical hydrogen-helium atmosphere of Jupiter have been evaluated and the rate of cellular convective motion, which may account for the motion of the red spot, estimated.<sup>4</sup> The purpose of this note is to apply similar methods to the outer solid layers of Jupiter which are made of molecular hydrogen containing, presumably, some dissolved helium.<sup>2</sup> The problem appears to be rather analogous to that of terrestrial continental drift, which has been carefully analyzed by Turcotte and Oxburgh.<sup>5</sup> They have shown that the self-diffusion-controlled creep and the resulting convection in the mantle account well for the observed rate of drift  $u$ . The pertinent formula is

$$u = 0.142\lambda R^{2/3}d^{-1}\rho^{-1}C_p^{-1} \quad (1)$$

with  $R$ , the Rayleigh number, given by  $R = g\alpha\rho^2 \times C_p^{-1}\lambda^{-1}\eta^{-1}\text{grad}T$ , where  $g$  is the gravitational acceleration,  $\lambda$  is the thermal conductivity,  $\eta$  is the viscosity,  $d$  is the thickness of the convecting layer,  $\rho$  is the density,  $\alpha$  is the thermal expansion,  $C_p$  is the specific heat, and  $\text{grad}T$  is the average vertical temperature gradient. Equation (1) is valid under certain assumptions, the most important one being the Boussinesq approximation which requires that except for the density all other parameters are constant. This condition implies that the depth  $d$  must be relatively small. Here  $R > R_c$  where  $R_c$ , the critical Rayleigh number, indicates the onset of convection.

Among the various quantities which enter into

the above formula viscosity and thermal conductivity require a careful consideration even for pure molecular hydrogen. Herring's theory of diffusion-controlled creep<sup>6</sup> permits estimating viscosity from an extrapolation<sup>2</sup> of experimental NMR self-diffusion data for solid molecular hydrogen to the appropriate regime of temperatures (below about 2000°K) and pressures (about  $10^{11}$  dyn cm<sup>-2</sup>). Within a factor of 20 the result is  $\eta = 10^{18}$  stokes. The considerable uncertainty is caused not only by the large extrapolation but also by the poor knowledge of the macroscopic structure of the solid. The problem of thermal conductivity  $\lambda$  is connected with the possible electronic and radiative contributions at elevated temperatures. The band gap in solid molecular hydrogen is about 10 eV and one expects it to go to zero when hydrogen becomes metallic at a pressure of  $(2-3) \times 10^{12}$  dyn cm<sup>-2</sup>. At the boundary between solid and liquid molecular hydrogen the pressure is about 10 times lower and so the band gap is still very large compared with the energy of thermal radiation corresponding to the ambient temperature. One would thus not expect much electronic contribution either to thermal conductivity or to the absorption of the thermal radiation. The propagation of the latter would be inhibited mainly by all kinds of scattering and by impurity absorption. Although there are some data<sup>7</sup> on high-temperature radiative heat transport in various ionic crystals such as oxides, as well as in crystals which are primarily covalent, there are no such data available for molecular high-band-gap crystals. From the existing observations one can expect that in the temperature region of interest the radiative heat transport in solid molecular hydrogen will be at most equal to the phonon contribution. The latter as estimated from the Leibfried-Schlömann formula<sup>8</sup>